Passivity Enforcement With Relative Error Control

Passivity Enforcement With Relative Error Control

Stefano Grivet-Talocia, *Senior Member, IEEE*, and Andrea Ubolli

***Abstract*—This paper introduces a new error control strategy in passivity enforcement schemes for linear lumped macromodels. We consider the general class of *a posteriori* passivity enforcement algorithms based on Hamiltonian matrix perturbation. Standard available formulations preserve the accuracy during passivity enforcement using special matrix norms associated to the controllability Gramian of the macromodel. This procedure leads to absolute error control. On the other hand, it is well known that relative error control in the macromodel is sometimes preferable, especially for structures that are characterized by small coupling coefficients or high dynamic range in their responses. Here, we present a frequency-weighting scheme leading to the definition of a modified Gramian that, when employed during passivity enforcement, effectively leads to relative error control. Several examples illustrate the reliability of the proposed technique.**

***Index Terms*—Hamiltonian matrices, linear macromodeling, passivity, perturbation theory, relative error, weighted Gramian.**

I. Introduction

PASSIVE macromodeling has become a common practice in the design flow of digital, RF, and mixed-signal systems in several application areas. Macromodeling techniques derive broadband equivalent circuits from frequency- or time-domain responses, typically obtained from full-wave field solvers or direct measurements. Such equivalent circuits can be used within standard circuit analysis tools such as SPICE in order to assess the electrical performance of a design since its early stages [1], [2]. Thus, macromodeling bridges the gap between fields and circuits, allowing their fast and accurate co-simulation.

Macromodels usually consist of Laplace-domain rational approximations of the transfer matrix of a given linear structure. Several algorithms are now available for the robust computation of these rational approximations starting from port responses. A very effective algorithm is the well-known *vector-fitting* scheme, in its various implementations [3]–[9]. This algorithm has now become *de facto* an industry standard, leading to more accurate and robust results with respect to its classical counterparts.

One of the important features that vector fitting (as well as many other common rational approximation schemes) is not able to guarantee is the passivity of the macromodel. A model is passive when it is unable to generate energy in any termination condition [10]–[13]. It is well known that nonpassive models may lead to unstable transient simulation depending on their termination networks [14], [15]. Thus, passivity is a fundamental property that should be enforced in any model for its safe use in a computer-aided design (CAD) environment. Even when beginning from initially passive data, rational macromodels may lack passivity for two main reasons. First, the unavoidable approximation errors may lead to passivity violations at those frequencies where the structure exploits a nearly lossless behavior. Second, the band-limited nature of any characterization (frequency or time domain, simulated or measured) does not allow controlling the behavior of the approximation outside the available data bandwidth. Therefore, the most severe passivity violations are usually located outside the desired modeling bandwidth.

Passivity has been a subject of intense research over the last few years. Several techniques are now available for the enforcement of macromodel passivity. Methods based on convex optimization [16], using some form of the positive real or bounded real lemma [13], do allow *a priori* passivity enforcement [17]–[19]. Their use is unfortunately limited to small-scale models both in terms of dynamic order and port count. *A posteriori* passivity correction techniques are available for larger size models. Some are based on linear or quadratic programming [15], [20]–[23] at discrete frequency samples. Other methods exploit the theory of Hamiltonian matrices [14], [24], [25]. We concentrate here on the latter class of methods, although the proposed formulation can be applied to any passivity enforcement scheme.

The above-mentioned *a posteriori* passivity enforcement schemes apply some perturbation to the model until its passivity is achieved. This perturbation is performed using special constraints insuring that the model accuracy is preserved. These constraints have always been formulated in terms of absolute error in the responses, except for the very recent results in [22], [26]–[28]. In this study, we present a method allowing for the systematic preservation of the relative error on each individual response during the passivity enforcement. We show that the proposed technique, which is based on a particular norm employing a frequency-weighted controllability Gramian of the model, leads to superior performance with respect to standard absolute error controlled schemes. This paper extends and generalizes the preliminary results presented in [28], where a simplified formulation is developed for one-port (scalar) models and applied only to low-complexity examples. Here, we present a complete and general formulation, including detailed derivations. The results in this study are directly applicable to macromodels with an arbitrary number of ports, as documented by the rich set of numerical examples taken from various application areas.

This paper is organized as follows. Section II motivates this study using a simple, but illustrative example. Section III introduces basic notation and background material. Section IV defines the frequency-weighted norms allowing for relative

Manuscript received April 24, 2007; revised July 23, 2007.

The authors are with the Department of Electronics, Politecnico di Torino, Turin 10129, Italy (e-mail: stefano.grivet@polito.it; andrea.ubolli@polito.it).

Color versions of one or more of the figures in this paper are available online at http://ieeexplore.ieee.org.

Digital Object Identifier 10.1109/TMTT.2007.908661

error control. Section V presents the new passivity enforcement scheme. Finally, Section VI demonstrates the excellent performance of proposed scheme on several examples.

II. Motivations

We motivate the need for relative error control using a very simple, but significant example. We consider the dc response of two coupled interconnects for digital signal transmission. The two signal lines have a dc resistance $R_w = 1\ \Omega$ and are referenced to a common larger ground conductor having dc resistance $R_g = 0.1\ \Omega$. The four-port scattering matrix referenced to $R_0 = 50\ \Omega$ is computed and successively used to evaluate the dc response of the interconnect. In this experiment, the near-end ports are matched, with an additional unit voltage source exciting only one conductor, and the two far-end ports are left open. Nominal dc solution is 1 V at both ports of the excited conductor, and 0 V on the victim conductor.

The nominal scattering matrix is then perturbed in two different ways. First, a constant perturbation is applied by adding $\varepsilon = 10^{-3}$ to all its elements, thus simulating the derivation of a macromodel with absolute error control. Relative perturbation is also applied by multiplying all elements by $(1+\varepsilon)$, thus simulating macromodel derivation with relative error control. The solution of the two models leads to a maximum 4-mV crosstalk offset in the absolute perturbation case, whereas this offset is as low as 1 μV in the relative perturbation case. This difference is mainly due to the change in the terminations with respect to the nominal (matched) conditions. Since any macromodel is meant to represent the port behavior of a linear structure under any possible termination scheme, it is clear that relative error control provides the optimal solution. Absolute error control may produce unreliable results.

III. Preliminaries and Notation

The main notation that will be used throughout this paper is introduced here. Reference material on Hamiltonian-based passivity enforcement schemes is also briefly recalled in order to simplify the presentation of the new developments in Section V.

A. Basic Notation

Throughout this paper, x, $\boldsymbol{x}$, and $\mathbf{X}$ denote a generic scalar, vector (lower case and boldface), and matrix (upper case and boldface), respectively. Superscripts *, ^{T}, and ^{H} will stand for the complex conjugate, transpose, and conjugate (Hermitian) transpose, respectively.

We consider linear macromodels in state–space form, described by the following standard shorthand notation:

$$\mathbf{H}(s) = \mathbf{D} + \mathbf{C}\,(s\mathbf{I} - \mathbf{A})^{-1}\,\mathbf{B} \leftrightarrow \left[\begin{array}{c|c} \mathbf{A} & \mathbf{B} \\ \hline \mathbf{C} & \mathbf{D} \end{array}\right] \tag{1}$$

where s is the Laplace variable, $\mathbf{H}(s)$ is the $p \times p$ transfer matrix of the macromodel, and $\{\mathbf{A}, \mathbf{B}, \mathbf{C}, \mathbf{D}\}$ are the state–space matrices of some realization associated to $\mathbf{H}(s)$. This macromodel is obtained via some fitting, approximation, or identification process from tabulated responses of a given linear and time-invariant structure or component. As an example, if $\{\mathbf{S}(j\omega_k), k = 1, \ldots, K\}$ are the frequency samples of the scattering matrix of the linear component over a given bandwidth, the macromodel parameters $\{\mathbf{A}, \mathbf{B}, \mathbf{C}, \mathbf{D}\}$ are obtained by solving

$$\min \|\mathbf{H}(j\omega_k) - \mathbf{S}(j\omega_k)\| \qquad \forall\, k \tag{2}$$

with a suitably defined norm. Several algorithms are available for this task, including the well-known vector-fitting scheme [3]–[9]. Note that any equivalent macromodel form in terms of poles/residues or poles/zeros is readily converted into (1).

We will assume a state–space realization with the same structure as in [14] since macromodels are usually obtained in this form [3], [5], [9]. More precisely, we assume the following structure:

$$\begin{aligned} \mathbf{A} &= \mathrm{blkdiag}\{\boldsymbol{\Lambda}_k, k = 1, \ldots, p\} \\ \mathbf{B} &= \mathrm{blkdiag}\{\boldsymbol{u}_k, k = 1, \ldots, p\} \\ \mathbf{C} &= [\mathbf{C}_1, \mathbf{C}_2, \ldots, \mathbf{C}_p] \end{aligned} \tag{3}$$

where $\boldsymbol{\Lambda}_k \in \mathbb{R}^{m_k \times m_k}$ stores in its diagonal the m_k poles of the kth column of $\mathbf{H}(s)$, $\boldsymbol{u}_k$ is a $m_k \times 1$ array with all entries equal to 1, and $\mathbf{C}_k \in \mathbb{R}^{p \times m_k}$ stores the residues of the kth column of $\mathbf{H}(s)$. If complex pole pairs are present, the transformation in [14] can be applied to the relevant blocks of (3) in order to recover a real realization. Therefore, we will assume a real-valued realization without loss of generality.

We will consider $\mathbf{H}(s)$ to be either a scattering or a hybrid matrix of the model, the latter also including impedance and admittance as special cases. A system in the form of (1) is passive when the following three conditions are fulfilled [12], [13].

1) Each element of $\mathbf{H}(s)$ is defined and analytic in $\mathbb{R}\mathrm{e}\{s\} > 0$.
2) $\boldsymbol{\Phi}(s) \geq 0$, $\forall\ s : \mathbb{R}\mathrm{e}\{s\} > 0$, where $\boldsymbol{\Phi}(s) = \mathbf{H}^H(s) + \mathbf{H}(s)$ in the hybrid representation case, and $\boldsymbol{\Phi}(s) = \mathbf{I} - \mathbf{H}^H(s)\mathbf{H}(s)$ in the scattering representation case.
3) $\mathbf{H}(s^*) = \mathbf{H}^*(s)$.

In the following, we will assume a slightly more stringent regularity condition than 1) by requiring all eigenvalues of $\mathbf{A}$ to be strictly stable. No purely imaginary poles will be allowed in the model. Conversely, we will not consider the overly restrictive strict passivity conditions [29] instead of 2) since we want to also include in our applications lossless structures.

Basic operations on transfer matrices can be recast as algebraic operations on the associated state–space realizations. In particular, we have

$$\mathbf{H}^{-1}(s) \leftrightarrow \left[\begin{array}{c|c} \mathbf{A} - \mathbf{B}\mathbf{D}^{-1}\mathbf{C} & -\mathbf{B}\mathbf{D}^{-1} \\ \hline \mathbf{D}^{-1}\mathbf{C} & \mathbf{D}^{-1} \end{array}\right] \tag{4}$$

whenever $\mathbf{D}$ is nonsingular, and

$$\mathbf{H}_1(s)\mathbf{H}_2(s) \leftrightarrow \left[\begin{array}{cc|c} \mathbf{A}_1 & \mathbf{B}_1\mathbf{C}_2 & \mathbf{B}_1\mathbf{D}_2 \\ \mathbf{0} & \mathbf{A}_2 & \mathbf{B}_2 \\ \hline \mathbf{C}_1 & \mathbf{D}_1\mathbf{C}_2 & \mathbf{D}_1\mathbf{D}_2 \end{array}\right] \tag{5}$$

for any pair of transfer matrices with compatible dimensions. The reader is referred to [30] for further details.

The controllability Gramian $\mathbf{P} = \mathbf{P}^T$ associated to (1) is defined as the solution of the following Lyapunov equation [11]:

$$\mathbf{A}\mathbf{P} + \mathbf{P}\mathbf{A}^T + \mathbf{B}\mathbf{B}^T = \mathbf{0}. \tag{6}$$

We will postulate controllability, which follows implicitly from the adopted structure (3). Therefore, the Gramian $\mathbf{P}$ is strictly positive definite and admits the following Cholesky decomposition:

$$\mathbf{P} = \mathbf{K}^T\mathbf{K} \tag{7}$$

where $\mathbf{K}$ is upper triangular.

B. Absolute Norms

Let us assume that the macromodel (1) is not passive. Most passivity enforcement schemes that have been presented thus far [20]–[25] try to find a new passive model

$$\mathbf{H}_p(s) \leftrightarrow \left[\begin{array}{c|c} \mathbf{A} & \mathbf{B} \\ \hline \mathbf{C}+\delta\mathbf{C} & \mathbf{D} \end{array}\right] \tag{8}$$

by preserving the system poles and perturbing the associated residues, which are located in matrix $\mathbf{C}$. The numerical evaluation of $\delta\mathbf{C}$ is performed in order to keep the induced perturbation in the system response

$$\delta\mathbf{H}(s) = \mathbf{H}_p(s) - \mathbf{H}(s) \leftrightarrow \left[\begin{array}{c|c} \mathbf{A} & \mathbf{B} \\ \hline \delta\mathbf{C} & \mathbf{0} \end{array}\right] \tag{9}$$

as small as possible. The standard measure that is used to quantify this amount of perturbation is the $\mathcal{L}^2$ (energy) norm, defined as

$$\begin{aligned} \|\delta\mathbf{H}\|^2 &= \frac{1}{2\pi}\sum_{ik}\int_{-\infty}^{\infty}|\delta H_{ik}(j\omega)|^2 d\omega \\ &= \frac{1}{2\pi}\int_{-\infty}^{\infty}\|\delta\mathbf{H}(j\omega)\|_F^2 d\omega \end{aligned} \tag{10}$$

where $\|\cdot\|_F$ denotes the Frobenius norm. It is clear from the above definitions that $\|\delta\mathbf{H}\|$ can be regarded as a cumulative *absolute error* in the responses induced by the perturbation.

The controllability Gramian $\mathbf{P}$ turns out to be very useful for the evaluation of (10) since it can be shown [30] that

$$\|\delta\mathbf{H}\|^2 = \mathrm{tr}\{\delta\mathbf{C}\,\mathbf{P}\,\delta\mathbf{C}^T\} = \mathrm{tr}\{\mathbf{\Delta}\mathbf{\Delta}^T\} = \|\mathrm{vec}(\mathbf{\Delta})\|_2^2 \tag{11}$$

where tr is the matrix trace, operator $\mathrm{vec}(\cdot)$ stacks the columns of its matrix argument [31], [32], and where

$$\mathbf{\Delta} = \delta\mathbf{C}\,\mathbf{K}^T \tag{12}$$

represents the perturbation on the state–space matrix $\mathbf{C}$ in a coordinate system defined by $\mathbf{K}$.

C. Hamiltonian-Based Passivity Enforcement

We now recall the definition of the Hamiltonian matrix associated to (1). In the hybrid case, we have

$$\mathcal{N}_\alpha = \begin{bmatrix} \mathbf{A}+\mathbf{B}\mathbf{Q}_\alpha^{-1}\mathbf{C} & \mathbf{B}\mathbf{Q}_\alpha^{-1}\mathbf{B}^T \\ -\mathbf{C}^T\mathbf{Q}_\alpha^{-1}\mathbf{C} & -\mathbf{A}^T-\mathbf{C}^T\mathbf{Q}_\alpha^{-1}\mathbf{B}^T \end{bmatrix} \tag{13}$$

with $\mathbf{Q}_\alpha = (2\alpha\mathbf{I}-\mathbf{D}-\mathbf{D}^T)$, whereas in the scattering case, we have

$$\mathcal{M}_\gamma = \begin{bmatrix} \mathbf{A}-\mathbf{B}\mathbf{R}_\gamma^{-1}\mathbf{D}^T\mathbf{C} & -\gamma\mathbf{B}\mathbf{R}_\gamma^{-1}\mathbf{B}^T \\ \gamma\mathbf{C}^T\mathbf{S}_\gamma^{-1}\mathbf{C} & -\mathbf{A}^T+\mathbf{C}^T\mathbf{D}\mathbf{R}_\gamma^{-1}\mathbf{B}^T \end{bmatrix} \tag{14}$$

with $\mathbf{R}_\gamma = (\mathbf{D}^T\mathbf{D}-\gamma^2\mathbf{I})$ and $\mathbf{S}_\gamma = (\mathbf{D}\mathbf{D}^T-\gamma^2\mathbf{I})$. Let $\Omega = \{\omega_i\}$ denote the set of (simple) purely imaginary eigenvalues of $\mathcal{N}_0$ (hybrid) or $\mathcal{M}_1$ (scattering). It can be shown [24], [33] that the model is not passive whenever $\Omega \neq \emptyset$. Passivity can be recovered by perturbing these imaginary eigenvalues [14], [24], [34] until they move off the imaginary axis.

We now recall the main result of [24], which is the starting point for the new developments of this paper. Hamiltonian eigenvalue displacement is achieved by solving an inverse perturbation problem, i.e., by finding the $\delta\mathbf{C}$ corresponding to a desired eigenvalue perturbation. Using standard first-order expansions, the following linear constraint:

$$2\mathbb{R}\mathrm{e}\{\boldsymbol{v}_{i1}^T \otimes \boldsymbol{z}_i^H\}\mathrm{vec}(\delta\mathbf{C}) = -\mathbb{I}\mathrm{m}\{\boldsymbol{v}_i^H\mathbf{J}\boldsymbol{v}_i\}\delta\omega_i \tag{15}$$

is obtained for each eigenvalue to be perturbed. In this expression, $\delta\omega_i$ denotes the desired perturbation on the ith imaginary eigenvalue, $\otimes$ is the Kronecker matrix product [31], [32], matrix $\mathbf{J}$ is defined as

$$\mathbf{J} = \begin{bmatrix} \mathbf{0} & \mathbf{I} \\ -\mathbf{I} & \mathbf{0} \end{bmatrix} \tag{16}$$

and

$$\boldsymbol{v}_i = \begin{bmatrix} \boldsymbol{v}_{i1} \\ \boldsymbol{v}_{i2} \end{bmatrix} \tag{17}$$

is the right eigenvector of the Hamiltonian matrix associated to eigenvalue ω_i. Vector $\boldsymbol{z}_i$ is defined as

$$\boldsymbol{z}_i = -\mathbf{Q}_0^{-1}\mathbf{B}^T\boldsymbol{v}_{i2} - \mathbf{Q}_0^{-1}\mathbf{C}\boldsymbol{v}_{i1} \tag{18}$$

in the hybrid case and

$$\boldsymbol{z}_i = \mathbf{D}\mathbf{R}_1^{-1}\mathbf{B}^T\boldsymbol{v}_{i2} + \mathbf{S}_1^{-1}\mathbf{C}\boldsymbol{v}_{i1} \tag{19}$$

in the scattering case. Detailed derivations can be found in [24].

To summarize, passivity is enforced by iteratively finding a solution of the underdetermined system having (15) as its ith row. According to (11), the mean energy of the absolute perturbation in all responses can be minimized by performing the basis change (12) in (15)

$$2\mathbb{R}\mathrm{e}\{\left(\boldsymbol{v}_{i1}^T\mathbf{K}^{-1}\right) \otimes \boldsymbol{z}_i^H\}\mathrm{vec}(\mathbf{\Delta}) = -\mathbb{I}\mathrm{m}\{\boldsymbol{v}_i^H\mathbf{J}\boldsymbol{v}_i\}\delta\omega_i \tag{20}$$

and finding the minimum-norm solution of this underdetermined system using standard pseudoinverse methods [35].

IV. Weighted Gramians

Here we introduce the frequency-dependent weighting schemes and the associated norms that will be used for the relative error control during passivity enforcement in Section V.

A. General Weighting Schemes

We start by defining a general weighting matrix

$$\mathbf{W}(s) \leftrightarrow \left[\begin{array}{c|c} \mathbf{A}^w & \mathbf{B}^w \\ \hline \mathbf{C}^w & \mathbf{D}^w \end{array}\right] \tag{21}$$

which is used to define a weighted model perturbation

$$\begin{aligned} \delta\mathbf{H}^w(s) &= \delta\mathbf{H}(s)\mathbf{W}(s) \\ &\leftrightarrow \left[\begin{array}{cc|c} \mathbf{A} & \mathbf{B}\mathbf{C}^w & \mathbf{B}\mathbf{D}^w \\ \mathbf{0} & \mathbf{A}^w & \mathbf{B}^w \\ \hline \delta\mathbf{C} & \mathbf{0} & \mathbf{0} \end{array}\right] \\ &= \left[\begin{array}{c|c} \widehat{\mathbf{A}} & \widehat{\mathbf{B}} \\ \hline \widehat{\mathbf{C}} & \widehat{\mathbf{D}} \end{array}\right] \end{aligned} \tag{22}$$

where the state–space realization is readily obtained using (5). We denote as

$$\widehat{\mathbf{P}} = \begin{bmatrix} \mathbf{P}^w & \mathbf{P}_{12} \\ \mathbf{P}_{21} & \mathbf{P}_{22} \end{bmatrix} \tag{23}$$

the controllability Gramian associated to (22). By now applying (11) to (22), we can compute the weighted norm of the model perturbation

$$\|\delta\mathbf{H}\|_w^2 = \|\delta\mathbf{H}^w\|^2 = \mathrm{tr}\{\delta\mathbf{C}\,\mathbf{P}^w\delta\mathbf{C}^T\}. \tag{24}$$

This norm is formally identical to (11), differing only from the choice of the Gramian, which is extracted from the upper left block of (23). This type of weighted norm has been extensively used to define frequency-weighted model-order reduction schemes [30], [36].

As a particular case, we can set

$$\mathbf{W}(s) = \mathbf{H}^{-1}(s) \tag{25}$$

provided that $\mathbf{H}(s)$ is minimum phase [30] so that its inverse is strictly stable and the corresponding controllability Gramian is positive definite. When these conditions hold, the frequency-weighted norm (24) becomes the *relative error*. Unfortunately, the minimization of this error does not guarantee the minimization of the relative error on each individual element of matrix $\mathbf{H}(s)$, which is indeed our main goal. In Section IV-B, we present how this goal can be achieved.

B. Single-Element Inverse Weighting

Let us apply the above inverse weighting scheme to the perturbation of a single matrix element of the model

$$\Theta_{ik}(s) = \delta H_{ik}(s) H_{ik}^{-1}(s). \tag{26}$$

We can thus introduce the cumulative relative error, in the $\mathcal{L}^2$ sense, as

$$\begin{aligned} \|\delta\mathbf{H}\|_r^2 &= \frac{1}{2\pi}\sum_{ik}\int_{-\infty}^{\infty} |\Theta_{ik}(j\omega)|^2 d\omega \\ &= \frac{1}{2\pi}\int_{-\infty}^{\infty} \|\boldsymbol{\Theta}(j\omega)\|_F^2 d\omega \end{aligned} \tag{27}$$

where $\boldsymbol{\Theta}(s)$ is a $p\times p$ matrix whose entries are constructed using (26). The remainder of this section is devoted to the algebraic characterization of the above relative norm in a form that is compatible with (11) and (20).

We begin by rearranging the elements of $\boldsymbol{\Theta}(s)$ in a single-column vector by stacking its columns

$$\boldsymbol{\theta}(s) = \mathrm{vec}(\boldsymbol{\Theta}(s)). \tag{28}$$

Equivalently,

$$\theta_\nu(s) = \Theta_{ik}(s) \tag{29}$$

where

$$\nu = \nu(i,k) = i + (k-1)p \tag{30}$$

and

$$k = k(\nu) = 1 + \left\lfloor \frac{(\nu-1)}{p} \right\rfloor \tag{31}$$

$$i = i(\nu) = 1 + \mathrm{rem}(\nu - 1, p) \tag{32}$$

where the $\lfloor\cdot\rfloor$ operator rounds its argument towards zero and rem denotes the remainder after integer division. The above indexing equivalence will be used throughout this section. Now by using the global realization (1) of $\mathbf{H}(s)$, we can easily extract a partial state-space realization for one of its elements

$$H_{ik}(s) \leftrightarrow \left[\begin{array}{c|c} \mathbf{A}_\nu & \mathbf{b}_\nu \\ \hline \mathbf{c}_\nu & d_\nu \end{array}\right] \tag{33}$$

where $\mathbf{A}_\nu = \boldsymbol{\Lambda}_{k(\nu)} \in \mathbb{R}^{n_\nu\times n_\nu}$ collects the n_ν poles of $H_{ik}(s)$, $\mathbf{b}_\nu = \boldsymbol{u}_{k(\nu)} \in \mathbb{R}^{n_\nu\times 1}$, $\mathbf{c}_\nu \in \mathbb{R}^{1\times n_\nu}$ is the $i(\nu)$th row of $\mathbf{C}_{k(\nu)}$, and d_ν is a scalar. Similarly, we have

$$\delta H_{ik}(s) \leftrightarrow \left[\begin{array}{c|c} \mathbf{A}_\nu & \mathbf{b}_\nu \\ \hline \delta\mathbf{c}_\nu & 0 \end{array}\right] \tag{34}$$

We now make the important assumption that $H_{ik}(s)$ is minimum phase so that its inverse $H_{ik}^{-1}(s)$ is strictly stable. This restriction will be removed in Section IV-C. This allows us to derive, using (4) and (5),

$$\theta_\nu(s) \leftrightarrow \left[\begin{array}{cc|c} \mathbf{A}_\nu & \mathbf{b}_\nu d_\nu^{-1}\mathbf{c}_\nu & \mathbf{b}^\nu d_\nu^{-1} \\ \mathbf{0} & \mathbf{A}_\nu - \mathbf{b}_\nu d_\nu^{-1}\mathbf{c}_\nu & -\mathbf{b}^\nu d_\nu^{-1} \\ \hline \delta\mathbf{c}_\nu & \mathbf{0} & \mathbf{0} \end{array}\right]. \tag{35}$$

Using (24), this partial state–space realization leads to

$$\frac{1}{2\pi}\int_{-\infty}^{\infty} |\theta_\nu(j\omega)|^2 d\omega = \mathrm{tr}\left\{\delta\mathbf{c}_\nu\mathbf{P}_\nu\delta\mathbf{c}_\nu^T\right\} = \delta\mathbf{c}_\nu\mathbf{P}_\nu\delta\mathbf{c}_\nu^T \tag{36}$$

where the single-element weighted Gramian $\mathbf{P}_\nu$ is computed as in (22) and (23) and is positive definite by construction. We can, therefore, perform the change of variable

$$\boldsymbol{\xi}_\nu = \delta\mathbf{c}_\nu\mathbf{U}_\nu^T \tag{37}$$

where

$$\mathbf{P}_\nu = \mathbf{U}_\nu^T\mathbf{U}_\nu \tag{38}$$

is the Cholesky decomposition of $\mathbf{P}_\nu$. Expression (36) becomes

$$\frac{1}{2\pi}\int_{-\infty}^{\infty}|\theta_\nu(j\omega)|^2 d\omega = \mathrm{tr}\left\{\boldsymbol{\xi}_\nu\boldsymbol{\xi}_\nu^T\right\} = \|\boldsymbol{\xi}_\nu\|_2^2. \quad (39)$$

The final step is to now compute the global relative error (27) by adding the energy contributions from all matrix elements. We have

$$\|\delta\mathbf{H}\|_r^2 = \sum_\nu \|\boldsymbol{\xi}_\nu\|_2^2 = \|\boldsymbol{\xi}\|_2^2 \quad (40)$$

where

$$\boldsymbol{\xi} = \left[\boldsymbol{\xi}_1, \boldsymbol{\xi}_2, \ldots, \boldsymbol{\xi}_{p^2}\right]^T. \quad (41)$$

It is clear from the above derivation that minimization of (40) corresponds to the minimization of the global energy of the relative perturbations on the model responses.

C. Minimum Phase Enforcement

We now remove the constraint that each element of the model should be minimum phase. Let us begin from (33). If $H_{ik}(s)$ is not minimum phase, it can be decomposed as

$$H_{ik}(s) = H_{ik}^m(s)H_{ik}^{\mathrm{ap}}(s) \quad (42)$$

where $H_{ik}^m(s)$ is minimum phase and $H_{ik}^{\mathrm{ap}}(s)$ is an all-pass function. This decomposition can be obtained as a particular case of a general result on inner–outer factorizations [37]. More precisely, if $\mathbf{X}$ is the solution of the following algebraic Riccati equation:

$$\mathbf{X}(\mathbf{A}_\nu - \boldsymbol{\beta}_\nu\mathbf{c}_\nu) + (\mathbf{A}_\nu - \boldsymbol{\beta}_\nu\mathbf{c}_\nu)^T\mathbf{X} - \mathbf{X}\boldsymbol{\beta}_\nu\boldsymbol{\beta}_\nu^T\mathbf{X} = 0 \quad (43)$$

where $\boldsymbol{\beta}_\nu = \mathbf{b}_\nu/d_\nu$, the minimum-phase factor has the following state-space realization:

$$H_{ik}^m(s) \leftrightarrow \left[\begin{array}{c|c} \mathbf{A}_\nu & \mathbf{b}_\nu \\ \hline \widetilde{\mathbf{c}}_\nu & d^\nu \end{array}\right] \quad (44)$$

where

$$\widetilde{\mathbf{c}}_\nu = \mathbf{c}_\nu + \boldsymbol{\beta}_\nu^T\mathbf{X}. \quad (45)$$

Therefore, a strictly stable and minimal realization of $\theta_\nu(s)$ is readily obtained by replacing $\mathbf{c}_\nu$ in (35) with $\widetilde{\mathbf{c}}_\nu$. Since, by construction,

$$\left|\delta H_{ik}(j\omega)H_{ik}^{-1}(j\omega)\right| = \left|\delta H_{ik}(j\omega)\left[H_{ik}^m(j\omega)\right]^{-1}\right| \qquad \forall\,\omega \quad (46)$$

the cumulative relative error in (27) is not affected by this substitution. With this modification, however, the partial weighted Gramian $\mathbf{P}_\nu$ results strictly positive definite and can be used to define the relative norms (36) and (40).

V. Passivity Enforcement With Relative Error Control

Here, we consider the linear constraints imposed by the Hamiltonian eigenvalue perturbation (15), and we illustrate the modifications that are needed for the implementation of (40) as a relative perturbation error control. First, we note that

$$\delta\mathbf{c} = \left[\delta\mathbf{c}_1, \delta\mathbf{c}_2, \ldots, \delta\mathbf{c}_{p^2}\right]^T \quad (47)$$

is simply a reordering of the elements in the overall perturbation $\delta\mathbf{C}$ of (9). Therefore, we can find a permutation matrix $\mathbf{T}$ such that

$$\delta\mathbf{c} = \mathbf{T}\mathrm{vec}(\delta\mathbf{C}). \quad (48)$$

Now using (37) and defining

$$\mathbf{U} = \mathrm{blkdiag}_\nu\{\mathbf{U}_\nu\} \quad (49)$$

we can write

$$\boldsymbol{\xi} = \mathbf{U}\mathbf{T}\mathrm{vec}(\delta\mathbf{C}). \quad (50)$$

Direct substitution into (15) leads to

$$\left[2\mathbb{R}\mathrm{e}\left\{\boldsymbol{v}_{i1}^T \otimes \boldsymbol{z}_i^H\right\}\mathbf{T}^T\mathbf{U}^{-1}\right]\boldsymbol{\xi} = -\mathbb{I}\mathrm{m}\left\{\boldsymbol{v}_i^H\mathbf{J}\boldsymbol{v}_i\right\}d\omega_i. \quad (51)$$

According to (40), the minimum-norm solution of this underdetermined system realizes a passivity enforcement scheme with relative error control on each individual response of the model.

We note that the form of (51) is practically identical to its counterpart (20) with absolute error control. A different coordinate change, (37) instead of (12), leads to a slightly different way in which the system rows are constructed, but the computational cost required for solving either system is identical. We remark that this cost is negligible with respect to the more demanding determination of the imaginary Hamiltonian eigenvalues and eigenvectors. This issue has already been addressed in [14] and [25]. Finally, we note that the traditional scheme with absolute error control requires the evaluation of the controllability Gramian $\mathbf{P}$ of the entire system (1), whereas the proposed scheme involves the evaluation of p^2 independent and small-size Gramians $\mathbf{P}_\nu$, one for each response. Given the diagonal structure of the adopted state–space realization of the model (3), this cost is negligible [14]. This applies to the solution of the algebraic Riccati equation (43) as well due to the small size of (33).

VI. Examples

The advantages of the proposed passivity enforcement scheme are illustrated here via several examples. The first synthetic example of Section VI-A is specifically designed to highlight the performance between different error control schemes. The other case studies are taken from various application areas in order to demonstrate the wide applicability of the proposed technique. Examples range from antennas (Section VI-B) to connectors (Section VI-C) and packages (Section VI-D).

A. Validation Test Case

The first example we consider is a synthetic three-port lumped structure (with 36 poles) that was specifically designed to compare the performance of the various passivity enforcement schemes. A similar test case was considered in [28],

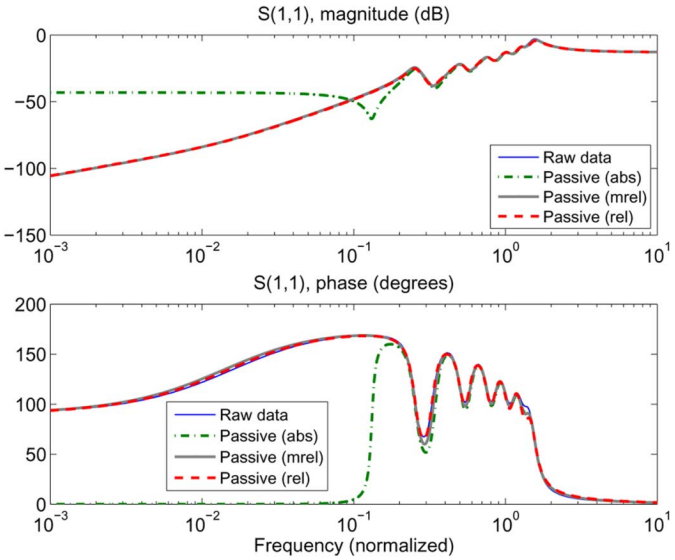

Fig. 1. Example VI-A (synthetic validation example). Responses of different passive models are compared to raw frequency data.

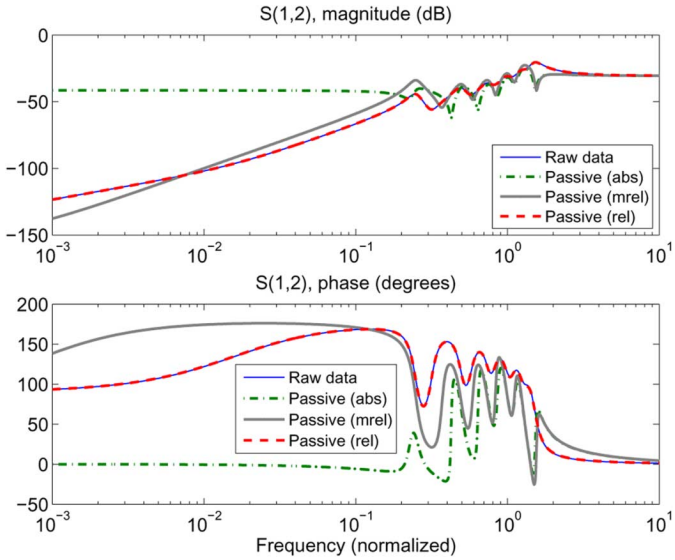

Fig. 2. Example VI-A (synthetic validation example). Responses of different passive models are compared to raw frequency data.

where the same procedure was applied to construct one of the numerical tests. The present example is a different realization of the same random generation process, briefly described below. First, poles of each response are defined as $p_k = -\alpha_k \pm j\beta_k$, where β_k are random variables uniformly distributed in the desired bandwidth and $\alpha_k/\beta_k = \rho$. A constant ratio $\rho = 0.1$ is used in this example. Placement of zeros follows the same process, with one additional real zero placed very close to the origin in order to force a small magnitude for some of the responses. Finally, the resulting rational scattering matrix $\mathbf{S}(s)$ is constrained via suitable scaling to have a maximum singular value $\sigma_{\max} = 1.2$. Note that the explicit placement of zeros guarantees that the model is minimum phase.

Three different passivity enforcement schemes were applied to this example. In all cases, passivity is enforced by iterative perturbation of Hamiltonian eigenvalues, as in [24], and as recalled in Section III-C. Each different scheme implements a different norm in order to control the accuracy during the model perturbation. Labeling of these options will be consistent throughout this section, namely,

- **abs** this is the standard scheme as in [24], expressed by the perturbation (20) associated with the absolute error control (11);
- **mrel** this scheme employs a matrix-based relative weighting scheme of (25), with a corresponding relative norm expressed by (24);
- **rel** this is our proposed scheme with relative error control on each individual response, expressed by (51).

The results are shown in Figs. 1 and 2 for two different matrix elements. A logarithmic scale is used in all plots in order to visualize clearly the relative errors on each response. As expected, the standard passivity scheme with absolute error control is limited in its resolution and fails in retaining a good accuracy for the small low-frequency values of each response. This means

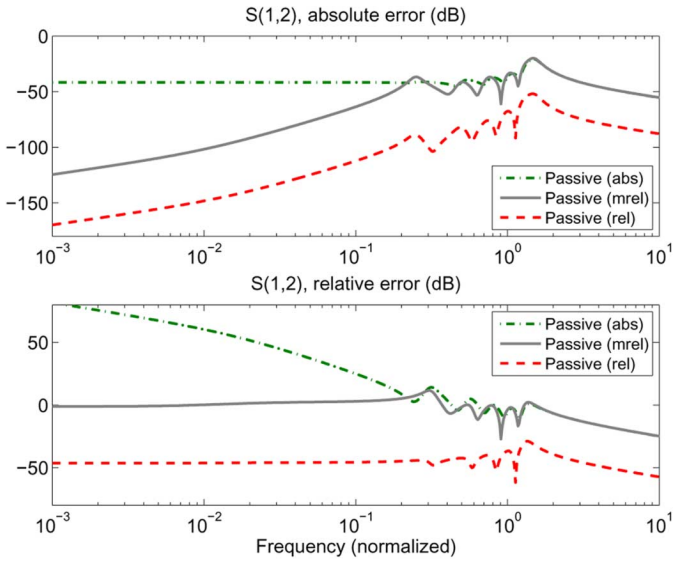

Fig. 3. Example VI-A (synthetic validation example). Absolute and relative errors of different passive models.

that the necessary perturbation that is needed to eliminate the passivity violation at a well-defined and limited frequency band has dramatic impact on the accuracy of the model at all frequencies. Although in absolute scale this may be acceptable for some applications, a better solution is indeed possible.

The second scheme with matrix-based relative error control achieves a better performance on S_{11}, but fails in retaining a good accuracy for S_{12}. This is also expected since this norm does not allow controlling individual responses. Finally, the proposed scheme guarantees excellent accuracy throughout the frequency bandwidth, even when the responses reach small values at low frequency. The only visible difference is concentrated around the largest peak, where the raw data are nonpassive. A better overview is provided in Fig. 3, where both absolute and relative errors are depicted for S_{12}. The relative error control clearly provides a better performance.

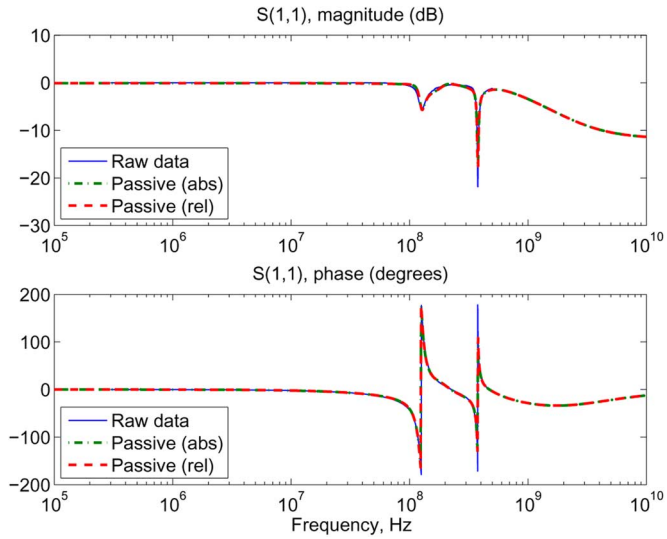

Fig. 4. Example VI-B (antenna–antenna coupling). Responses of different passive models are compared to raw frequency data.

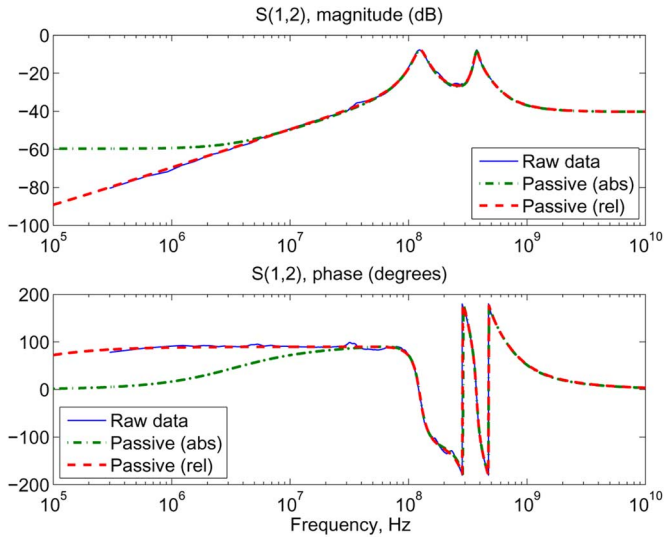

Fig. 5. Example VI-B (antenna–antenna coupling). Responses of different passive models are compared to raw frequency data.

B. Glass Antenna

The second example is a two-port model representing the mock-up of a double-feed glass antenna for automotive applications. The 2×2 scattering matrix of the structure has been measured at the antenna feed ports using a vector network analyzer (VNA). The investigated frequency band ranges from 300 kHz up to 500 MHz. A rational macromodel with 20 poles was generated using vector-fitting iterations with inverse weighting [4], [9]. This allows retaining good accuracy also for the off-diagonal scattering elements (feed-to-feed coupling). A passivity check on this initial macromodel shows small passivity violations (maximum singular value $\sigma_{\max} = 1.01$) in a small bandwidth centered between the two main resonances. The reason for this initial passivity violation is due to both noise in the original data and approximation error in the rational fitting stage.

Both passivity enforcement schemes with absolute and relative error control were applied to correct this small gain in the initial model, leading to the results of Figs. 4 and 5. Both schemes lead to excellent accuracy control for S_{11}. However, the performance is quite different for the coupling coefficient S_{12}. For this element, model quality is significantly deteriorated by the standard scheme, whereas the proposed new algorithm preserves a good accuracy at all frequencies.

C. Connector

The third example that we consider is a connector. As for Example VI-B, the four-port scattering matrix corresponding to the terminals of two adjacent pins was measured up to 20 GHz using a VNA. Small crosstalk values are found at low frequencies. We want to preserve such small couplings also in the passive model to be identified from the measured data. To this end, an initial rational macromodel was generated using vector-fitting iterations using inverse weighting, resulting in a state–space realization with 480 states. After having verified its lack of passivity (maximum singular value $\sigma_{\max} = 1.15$), this model was then processed by the passivity enforcement schemes with both absolute and relative error control in order to compare their performance.

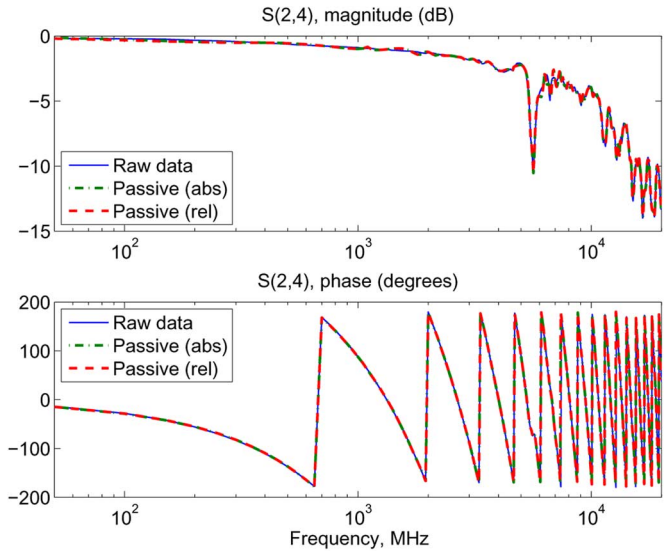

Fig. 6. Example VI-C (connector). Responses of different passive models are compared to raw frequency data.

The results are depicted in Figs. 6 and 7 for two elements of the scattering matrix. As for Example VI-B, the scheme based on relative error control closely matches the measured data, whereas the scheme based on absolute error control fails in the approximation of S_{22} at low frequencies.

D. Package

The last example is a complex package with 34 ports, including both signal and ground pins. The raw scattering responses are known from the results of an electromagnetic solver. As a preliminary study, we considered a subset of six ports and we generated the corresponding rational model consisting of a state–space realization of order 206. The challenge for this example is the very large dynamic range of some of the responses over a very large frequency range spanning ten decades. Two

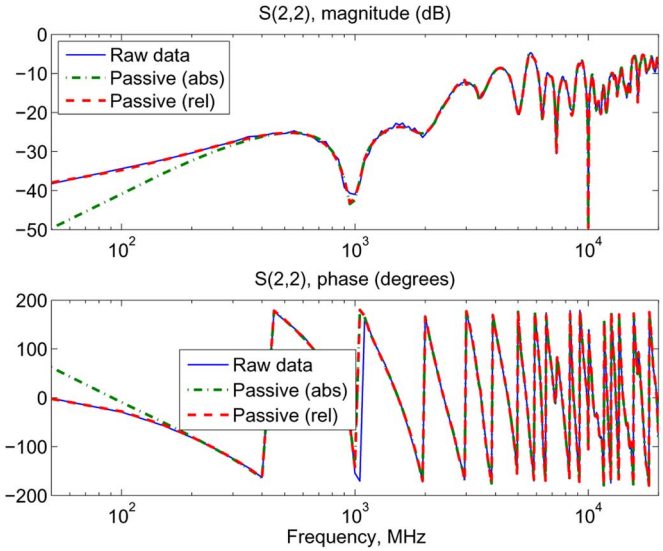

Fig. 7. Example VI-C (connector). Responses of different passive models are compared to raw frequency data.

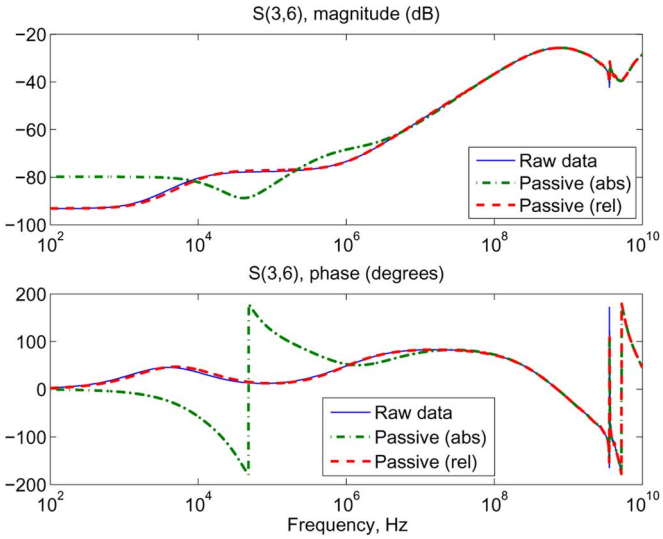

Fig. 8. Example VI-D (package). Responses of different passive models are compared to raw frequency data.

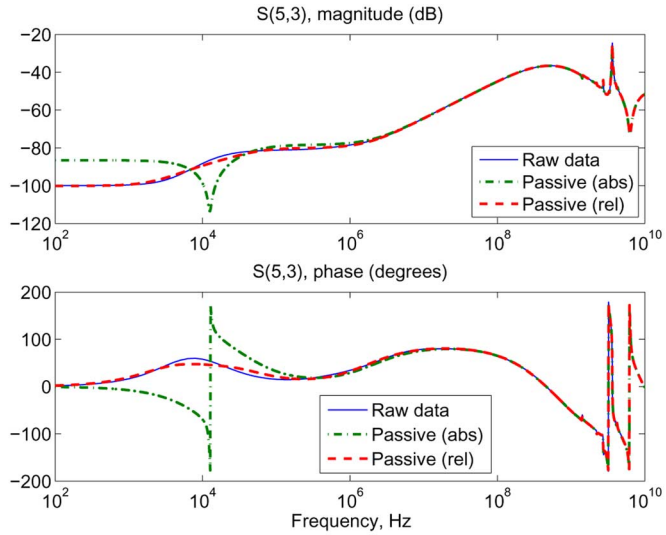

Fig. 9. Example VI-D (package). Responses of different passive models are compared to raw frequency data.

significant responses are depicted in Figs. 8 and 9. The rational model was generated using vector fitting with inverse weighting, as with the other cases, in order to preserve the nature of the small couplings, especially at dc. Passivity was then enforced using both absolute and relative error control. The results are compared in Figs. 8 and 9. The proposed scheme offers an excellent match to the raw data, whereas absolute error control is not able to preserve model accuracy at low frequencies.

VII. Discussion and Conclusions

In this study, we have suggested a general approach for the relative error minimization in passivity enforcement schemes, as opposed to standard absolute error control. We now put our study in perspective by comparing the approach to other existing passivity enforcement methods.

We begin by noting that any passivity enforcement scheme is based on two fundamental elements, i.e.: 1) the passivity constraints and 2) some accuracy metric. Here, we have mainly addressed the second issue, showing that existing approaches based on absolute error control may be inadequate for some applications. For instance, a noise analysis for structures that require very high isolation levels between some ports fails if the absolute error is used since the absolute perturbation induced on small responses might be orders of magnitude larger than the desired isolation level. For such applications, a relative error control strategy is preferred. This paper provides a solution for all applications subject to these accuracy constraints.

The proposed technique is, in principle, applicable to any formulation of the passivity constraints, including schemes based on the passivity enforcement at discrete frequency samples [15], [20]–[23] and schemes based on the solution of linear matrix inequalities (LMI) via convex optimization [17]–[19]. The latter are the only methods leading to the strictly optimal solution, where optimality depends, of course, on the adopted norm. Unfortunately, LMI-based schemes are not applicable in practical situations due to the overwhelming computational complexity, even for moderate model size.

The proposed method is based on iterative Hamiltonian first-order perturbation, which is only suboptimal: each iteration computes an optimal step towards the solution, but the final result might not be strictly the nearest to the original model in the adopted norm. However, the methodology is applicable to large-sized models with thousands of states [14], [25]. Therefore, one may be willing to trade a little accuracy for the ability to solve the problem. The numerical results show, however, an excellent performance of the Hamiltonian-based formulation in terms of accuracy.

For the proposed technique, the precise computation of the purely imaginary Hamiltonian eigenvalues is of paramount importance. This calculation is the most computationally demanding part of the overall scheme. The techniques proposed

in [14] provide fast algorithms for this evaluation based on multipoint restarted Arnoldi iterations. Further speedup might be obtained if the number of these eigenvalues could be estimated, e.g., using Gershgorin's theory [23], [34]. Unfortunately, application of these results to typical Hamiltonian spectra does not lead to useful estimates due to the lack of diagonal dominance. Therefore, estimates based on adaptive sampling [25] are preferred.

We conclude by pointing the reader to other ongoing research on passivity enforcement of macromodels. References [26] and [27] also use a Hamiltonian-based approach, but formulate the passivity enforcement as a nonlinear optimization using poles as free variables and imposing accuracy both in the absolute and matrix-relative sense at discrete frequency samples. Perturbing poles has the advantage of reducing the number of variables, but may be inapplicable in case of highly resonant structures, where the poles have a physical correspondence to the system resonances. Here, we explicitly preserve the system poles in order to avoid this difficulty. Reference [22] enforces passivity at discrete frequency samples, but using an innovative accuracy control strategy based on relative errors on residue matrix eigenvalues rather on matrix elements. This approach is best suited to stiff applications showing high sensitivity to terminations.

REFERENCES

[1] M. Celik, L. Pileggi, and A. Obadasioglu, *IC Interconnect Analysis*. Norwell, MA: Kluwer, 2002.

[2] M. Nakhla and R. Achar, "Simulation of high-speed interconnects," *Proc. IEEE*, vol. 89, no. 5, pp. 693–728, May 2001.

[3] B. Gustavsen and A. Semlyen, "Rational approximation of frequency responses by vector fitting," *IEEE Trans. Power Del.*, vol. 14, no. 3, pp. 1052–1061, Jul. 1999.

[4] B. Gustavsen, "Computer code for rational approximation of frequency dependent admittance matrices," *IEEE Trans. Power Del.*, vol. 17, no. 4, pp. 1093–1098, Oct. 2002.

[5] B. Gustavsen and A. Semlyen, "A robust approach for system identification in the frequency domain," *IEEE Trans. Power Del.*, vol. 19, no. 3, pp. 1167–1173, Jul. 2004.

[6] D. Deschrijver and T. Dhaene, "Rational modeling of spectral data using orthonormal vector fitting," in *Proc. 9th IEEE Signal Propag. Interconnects Workshop*, Garmisch-Partenkirchen, Germany, May 10–13, 2005, pp. 111–114.

[7] D. Deschrijver, B. Haegeman, and T. Dhaene, "Orthonormal vector fitting: A robust macromodeling tool for rational approximation of frequency domain responses," *IEEE Trans. Adv. Packag.*, vol. 30, no. 2, pp. 216–225, May 2007.

[8] S. Grivet-Talocia and M. Bandinu, "Improving the convergence of vector fitting in presence of noise," *IEEE Trans. Electromagn. Compat.*, vol. 48, no. 1, pp. 104–120, Feb. 2006.

[9] "IdEM 2.4," Politech. Torino, Turin, Italy, 2006. [Online]. Available: www.emc.polito.it

[10] V. Belevitch, *Classical Network Theory*. San Francisco, CA: Holden-Day, 1968.

[11] T. Kailath, *Linear Systems*. Englewood Cliffs, NJ: Prentice-Hall, 1980.

[12] M. R. Wohlers, *Lumped and Distributed Passive Networks*. New York: Academic, 1969.

[13] S. Boyd, L. El Ghaoui, E. Feron, and V. Balakrishnan, *Linear Matrix Inequalities in System and Control Theory*, ser. Studies in Appl. Math. Philadelphia, PA: SIAM, 1994.

[14] S. Grivet-Talocia and A. Ubolli, "On the generation of large passive macromodels for complex interconnect structures," *IEEE Trans. Adv. Packag.*, vol. 29, no. 1, pp. 39–54, Feb. 2006.

[15] D. Saraswat, R. Achar, and M. Nakhla, "Global passivity enforcement algorithm for macromodels of interconnect subnetworks characterized by tabulated data," *IEEE Trans. Very Large Scale Integr. (VLSI) Syst.*, vol. 13, no. 7, pp. 819–832, Jul. 2005.

[16] B. Stephen and V. Lieven, *Convex Optimization*. Cambridge, U.K.: Cambridge Univ. Press, 2004.

[17] C. P. Coelho, J. Phillips, and L. M. Silveira, "A convex programming approach for generating guaranteed passive approximations to tabulated frequency-data," *IEEE Trans. Comput.-Aided Design Integr. Circuits Syst.*, vol. 23, no. 2, pp. 293–301, Feb. 2004.

[18] H. Chen and J. Fang, "Enforcing bounded realness of S parameter through trace parameterization," in *12th IEEE Elect. Perform. Electron. Packag. Topical Meeting*, Princeton, NJ, Oct. 27–29, 2003, pp. 291–294.

[19] B. Dumitrescu, "Parameterization of positive-real transfer functions with fixed poles," *IEEE Trans. Circuits Syst. I, Fundam. Theory Appl.*, vol. 49, no. 4, pp. 523–526, Apr. 2002.

[20] B. Gustavsen and A. Semlyen, "Enforcing passivity for admittance matrices approximated by rational functions," *IEEE Trans. Power Syst.*, vol. 16, no. 1, pp. 97–104, Feb. 2001.

[21] B. Gustavsen, "Computed code for passivity enforcement of rational macromodels by residue perturbation," *IEEE Trans. Adv. Packag.*, vol. 30, no. 2, pp. 209–215, May 2007.

[22] B. Gustavsen, "Fast passivity enforcement of rational macromodels by perturbation of residue matrix eigenvalues," in *11th IEEE Signal Propag. Interconnects Workshop*, Ruta di Camogli, Genova, Italy, May 13–16, 2007, pp. 71–74.

[23] D. Saraswat, R. Achar, and M. Nakhla, "A fast algorithm and practical considerations for passive macromodeling of measured/simulated data," *IEEE Trans. Compon., Packag., Manuf. Technol.*, vol. 27, no. 1, pp. 57–70, Feb. 2004.

[24] S. Grivet-Talocia, "Passivity enforcement via perturbation of Hamiltonian matrices," *IEEE Trans. Circuits Syst. I, Fundam. Theory Appl.*, vol. 51, no. 9, pp. 1755–1769, Sep. 2004.

[25] S. Grivet-Talocia, "An adaptive sampling technique for passivity characterization and enforcement of large interconnect macromodels," *IEEE Trans. Adv. Packag.*, vol. 30, no. 2, pp. 226–237, May 2007.

[26] A. Lamecki and M. Mrozowski, "Passive SPICE networks from nonpassive data," in *16th Int. Microw., Radar, Wireless Commun. Conf.*, Krakow, Poland, May 22–24, 2006, vol. 3, pp. 981–983.

[27] A. Lamecki and M. Mrozowski, "Equivalent SPICE circuits with guaranteed passivity from nonpassive models," *IEEE Trans. Microw. Theory Tech.*, vol. 55, no. 3, pp. 526–532, Mar. 2007.

[28] S. Grivet-Talocia and A. Ubolli, "On relative error minimization in passivity enforcement schemes," in *11th IEEE Signal Propag. Interconnects Workshop*, Ruta di Camogli, Genova, Italy, May 13–16, 2007, pp. 75–78.

[29] L. Knockaert, "A note on strict passivity," *Syst. Control Lett.*, vol. 54, no. 9, pp. 865–869, Sep. 2005.

[30] K. Zhou, J. C. Doyle, and K. Glover, *Robust and Optimal Control*. Englewood Cliffs, NJ: Prentice-Hall, 1996.

[31] J. W. Brewer, "Kronecker products and matrix calculus in system theory," *IEEE Trans. Circuits Syst.*, vol. CAS-25, no. 9, pp. 772–781, Sep. 1978.

[32] C. F. V. Loan, "The ubiquitous Kronecker product," *J. Comput. Appl. Math.*, vol. 123, pp. 85–100, 2000.

[33] S. Boyd, V. Balakrishnan, and P. Kabamba, "A bisection method for computing the H_∞ norm of a transfer matrix and related problems," *Math. Control Signals Syst.*, vol. 2, pp. 207–219, 1989.

[34] J. H. Wilkinson, *The Algebraic Eigenvalue Problem*. London, U.K.: Oxford Univ. Press, 1965.

[35] MATLAB *Release 14 User's Guide*. Natick, MA: The MathWorks, 2006. [Online]. Available: www.mathworks.com,

[36] K. Zhou, "Frequency-weighted $\mathcal{L}^\infty$ norm and optimal Hankel norm model reduction," *IEEE Trans. Autom. Control*, vol. 40, no. 10, pp. 1687–1699, Oct. 1995.

[37] X. Chen and K. Zhou, "On the relative and multiplicative model reduction," in *Proc. 27th Southeastern Syst. Theory Symp.*, Mar. 12–14, 1995, pp. 57–60.

Stefano Grivet-Talocia (M'98–SM'07) received the Laurea and Ph.D. degrees in electronic engineering from the Politecnico di Torino, Turin, Italy, in 1994 and 1998, respectively.

From 1994 to 1996, he was with the National Aeronautics and Space Administration (NASA)/Goddard Space Flight Center, Greenbelt, MD, where he was involved with applications of fractal geometry and wavelet transform to the analysis and processing of geophysical time series. He is currently an Associate Professor of circuit theory with the Department of

Electronics, Politecnico di Torino. He has authored over 80 journal and conference papers. His current research interests are passive macromodeling of lumped and distributed interconnect structures, modeling and simulation of fields, circuits, and their interaction, wavelets, time-frequency transforms, and their applications.

Dr. Grivet-Talocia was an associate editor for the IEEE TRANSACTIONS ON ELECTROMAGNETIC COMPATIBILITY from 1999 to 2001.

Andrea Ubolli received the Laurea degree in electronic engineering from the Politecnico di Torino, Turin, Italy, in 2003, where he is currently working toward the Ph.D. degree.

Upon graduation, he has been with the Electromagnetic Compatibility (EMC) Group, Department of Electronics, Politecnico di Torino, as a Research Assistant. His research interests are in the field of electromagnetic compatibility, where he is involved with macromodeling of electrical interconnects and power integrity in microscale and macroscale complex interconnected systems, with an emphasis on passivity enforcement schemes.